Optical absorption spectra of Eu^{3+} in $Y_3Ga_5O_{12}$ (YGG)

1997 J. Phys.: Condens. Matter 9 1637

(http://iopscience.iop.org/0953-8984/9/7/025)

J. Phys.: Condens. Matter **9** (1997) 1637–1648. Printed in the UK PII: S0953-8984(97)75337-2

Optical absorption spectra of Eu^{3+} in $Y_3Ga_5O_{12}$ (YGG)

K Binnemans† and C Görller-Walrand

K U Leuven, Department of Chemistry, Coordination Chemistry Division, Celestijnenlaan 200F, B-3001 Heverlee, Belgium

Received 12 June 1996, in final form 31 October 1996

Abstract. Optical absorption spectra of trivalent europium in the rare-earth garnet $Y_3Ga_5O_{12}$ (YGG) have been recorded between 4600 and 32 000 cm^{-1} at 77 and at 293 K. A total of 117 crystal-field transitions has been detected in the spectra. The symmetry of the Eu^{3+} site is D_2, so a total removal of the crystal-field degeneracy of the $4f^6$ configuration can be expected. The energy level scheme of Eu^{3+} in YGG is parametrized in terms of 20 free-ion parameters and nine crystal-field parameters. The crystal field is strong in the garnet host, so J-mixing has to be taken into account for the crystal-field calculation.

1. Introduction

Rare-earth garnets are interesting materials for solid state lasers [1]. An overview of the spectroscopic properties of trivalent lanthanide ions in rare-earth garnets is given by Morrison and Leavitt [2]. Koningstein [3] has published the energy level scheme of $Y_3Ga_5O_{12}$:Eu^{3+} between 0 and 19 000 cm^{-1}. He has recorded the fluorescence spectrum in the spectral region from 12 000 to 16 950 cm^{-1} and the absorption spectrum between 1900 cm^{-1} in the infrared and 20 000 cm^{-1} in the visible part of the spectrum.

In this paper, we report the optical absorption spectra of Eu^{3+} in the rare-earth garnet $Y_3Ga_5O_{12}$ (YGG). The measurements span the 4600–32 000 cm^{-1} spectral region. The spectra have been recorded at 293 and at 77 K. The Eu^{3+} ion is attractive from a spectroscopic viewpoint, because of the non-degenerate ground state $^7F_0$ and because of the presence of several $^{2S+1}L_J$ manifolds with a small total angular momentum J. A distinct correlation between structural and spectroscopic properties is therefore possible. The energetic scheme of the $4f^6$ configuration is reconstructed and the energy levels are parametrized in terms of free-ion and crystal-field parameters. The symmetry at the rare-earth site is orthorhombic (D_2 symmetry). There are six crystallographically, but magnetically inequivalent D_2 sites per unit cell [4]. The consequence is that one can define six sets of crystal-field parameters which may appear to be completely different, but which give identical crystal-field splittings.

2. Experimental details

The Eu^{3+} doped $Y_3Ga_5O_{12}$ (YGG) single crystal was provided by G Blasse (University of Utrecht, The Netherlands). Approximately 10% of the Y^{3+} in YGG have been replaced

† Send correspondence to Dr K Binnemans, K U Leuven, Department of Chemistry, Coordination Chemistry Division, Celestijnenlaan 200F, B-3001 Heverlee (Leuven), Belgium.

0953-8984/97/071637+12$19.50

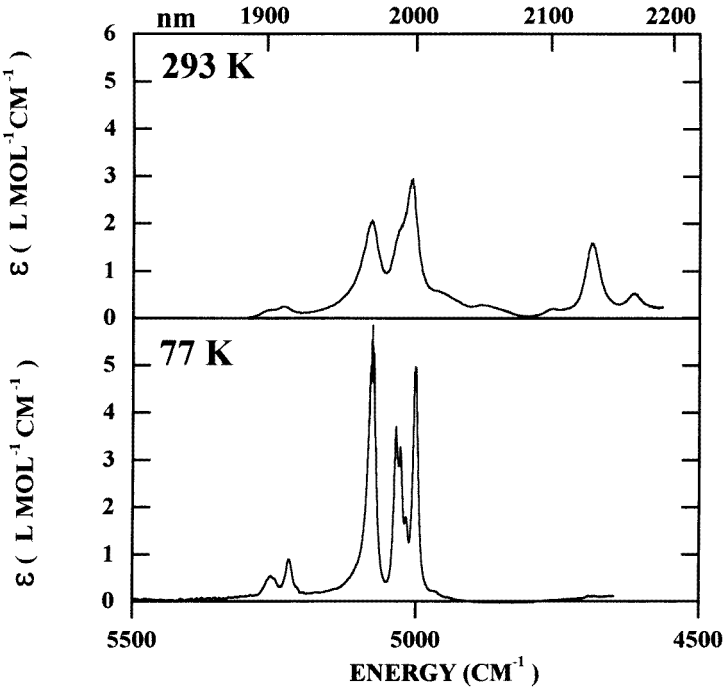

Figure 1. Absorption spectra of the transitions to $^7F_6$ in YGG:Eu^{3+} at 293 and at 77 K.

by Eu^{3+}. The YGG:Eu^{3+} crystal is colourless [5]. Absorption spectra were recorded on an AVIV 17DS spectrophotometer. The optics of the instrument are based on those of the Cary 17. It covers the ultraviolet, visible and near-infrared regions (185–2500 nm) with a double monochromator: a 30° fused silica prism and a 600 lines mm^{-1} grating. Resolution in most of the UV–VIS wavelength range is 0.07 nm. In the near infrared the resolution is about 0.3 nm. The wavelength reproducibility is within 0.05 nm in the UV–VIS and 0.25 nm in the near infrared. A spectral bandwidth of 0.05 nm in the visible and 2 nm in the infrared was used. The sample was cooled in a continuous flow cryostat (Oxford Instruments), with liquid nitrogen as refrigerant (77 K). Data collection is digital and processing is performed by commercial software on a PC.

3. Analysis of the spectra

In the near infrared, transitions to the $^7F_6$ multiplet are found (4600–5400 cm^{-1}) (figure 1). These transitions are intense, because they are spin allowed ($\Delta S = 0$). The transitions starting from the $^7F_1$ manifold can be observed only partially, because of instrumental restrictions. A peak at 16 406 cm^{-1} in the spectrum at ambient temperature can be assigned to the $^5D_0 \leftarrow ^7F_2$ transition. This is the only transition starting from the $^7F_2$ level in the YGG:Eu^{3+} crystal. Three peaks are found for the $^5D_0 \leftarrow ^7F_1$ transition at 293 K (16 820, 16 867 and 16 902 cm^{-1}). The total removal of the crystal-field degeneracy of the $^7F_1$ level indicates that the site symmetry in the garnet is orthorhombic or lower (figure 2). As mentioned above, the site has the orthorhombic D_2 symmetry. The $^5D_0 \leftarrow ^7F_0$ transition is forbidden in a D_2 symmetry and is indeed not observed in the absorption spectrum of

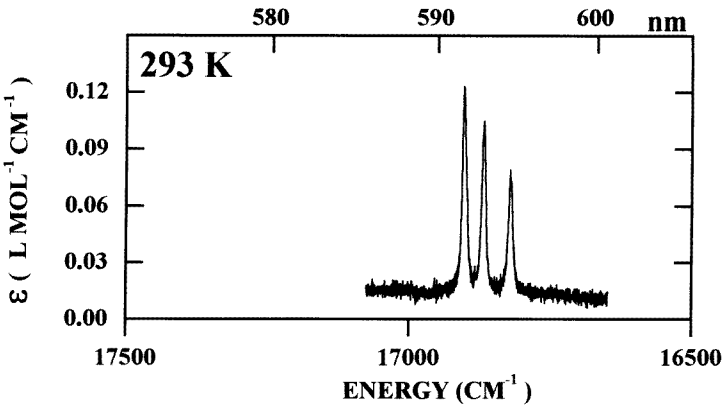

Figure 2. Absorption spectrum of the $^5D_0 \leftarrow ^7F_1$ transition in YGG:Eu^{3+} at 293 K.

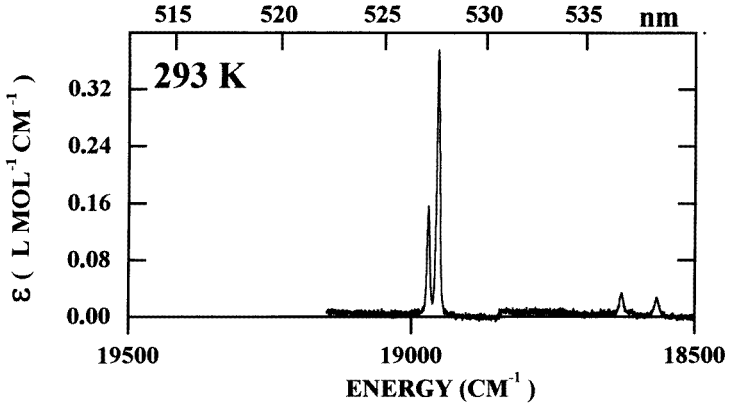

Figure 3. Absorption spectrum of the transitions to $^5D_1$ in YGG:Eu^{3+} at 293 K.

YGG:Eu^{3+}. The hypersensitive transition $^5D_1 \leftarrow ^7F_1$ is only weak. Two peaks are resolved well (18 567 and 18 627 cm^{-1}). Another one is observed as a shoulder at 18 611 cm^{-1} (figure 3). Although three peaks are expected for the $^5D_1 \leftarrow ^7F_0$ transition, only two are effectively found in the spectrum: 18 954 and 18 971 cm^{-1} (figure 3). Calculations show that the peak at 18 954 cm^{-1} consists in fact of two overlapping peaks. Those two peaks are not resolved in the absorption spectrum. Using the transitions $^5D_0 \leftarrow ^7F_1$, $^5D_1 \leftarrow ^7F_1$ and $^5D_1 \leftarrow ^7F_0$, it is possible to determine the energetic positions of the $^5D_0$ level and the crystal-field levels of the $^7F_1$ multiplet. Transitions to the $^5D_2$ multiplet are found between 21 000 and 21 500 cm^{-1} (figure 4). Three peaks are found for the transition $^5D_2 \leftarrow ^7F_0$, in agreement with the predictions for a D_2 symmetry: at 21 362, at 21 448 and at 21 471 cm^{-1}. The hypersensitive transition $^5D_2 \leftarrow ^7F_0$ (induced electric dipole transition) is less intense than the magnetic dipole transition $^5D_1 \leftarrow ^7F_0$. Five weak transitions in the 293 K spectrum can be assigned to the $^5D_2 \leftarrow ^7F_1$ transition. The next J-level of the ^5D term is $^5D_3$. In normal circumstances, the $^5D_3 \leftarrow ^7F_0$ transition (around 24 250 cm^{-1}) is not observed, because this transition ($\Delta J = 3$) is forbidden by the selection rules for induced electric

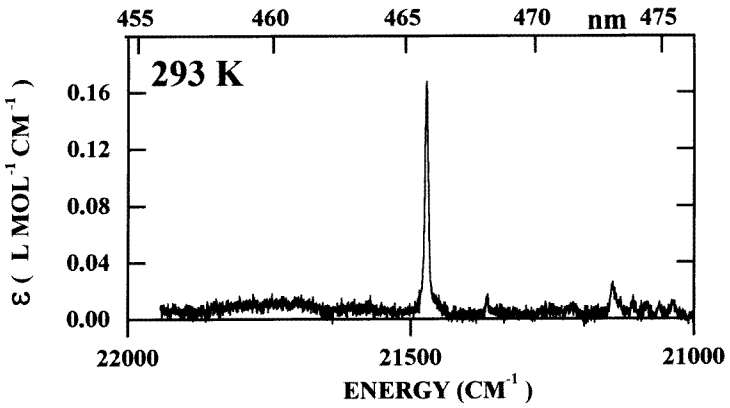

Figure 4. Absorption spectrum of the transitions to $^5D_2$ in YGG:Eu^{3+} at 293 K.

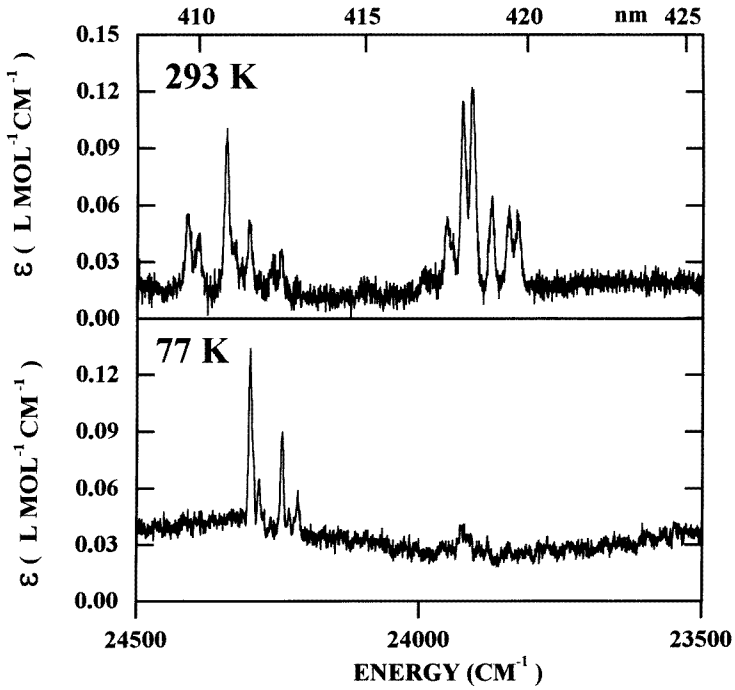

Figure 5. Absorption spectra of the transitions to $^5D_3$ in YGG:Eu^{3+} at 293 and at 77 K.

dipole transitions ($\Delta J = 2, 4$ and 6 for transitions starting from the $^7F_0$ level). In that case, the crystal-field levels of the $^5D_3$ multiplet have to be determined from the $^5D_3 \leftarrow {}^7F_1$ transition ($\Delta J = 2$). In YGG:Eu^{3+}, the $^5D_3 \leftarrow {}^7F_0$ transition is, however, observed. This is due to the strong J-mixing in the garnet host. J-mixing can relax the selection rule on ΔJ. The intensity of these crystal-field transitions is very low. They are found in the spectral region where also the $^5L_6 \leftarrow {}^7F_1$ transitions can be expected. The latter transitions will disappear when cooling the sample, while the intensity of the $^5D_3 \leftarrow {}^7F_0$ transition will

increase (depopulation of the $^7F_1$ level in favour of the $^7F_0$ level). Six peaks can be assigned to the $^5D_3 \leftarrow ^7F_0$ transition and also six to the $^5D_3 \leftarrow ^7F_1$ transition. In this way, six of the seven crystal-field levels of the $^5D_3$ manifold can be located (figure 5).

Transitions to the $^5L_6$ multiplet are the most intense transitions in the visible and ultraviolet part of the Eu^{3+} spectrum. Because of the large splitting of the $^5L_6$ manifold in YGG:Eu^{3+}, the $^5L_6 \leftarrow ^7F_0$ and $^5L_6 \leftarrow ^7F_1$ transitions overlap. Separation of the two transitions can be achieved by the fact that only the $^5L_6 \leftarrow ^7F_0$ transition is observed at 77 K. At this temperature, the rather broad crystal-field transitions of $^5L_6 \leftarrow ^7F_0$ are better resolved. Nine of the 13 crystal-field levels of the $^5L_6$ manifold have been detected experimentally. The total crystal-field splitting of the manifold is 731 cm^{-1}. The splitting of the $^5L_6$ multiplet is rather strange. The crystal-field levels of the multiplet are divided into two groups and separated by an energy gap of more than 500 cm^{-1}. The lower subgroup of six crystal-field levels is only about 70 cm^{-1} across, whereas the upper subgroup of seven crystal-field levels is spread over no more than 200 cm^{-1}. This is proved by crystal-field calculations (figure 6).

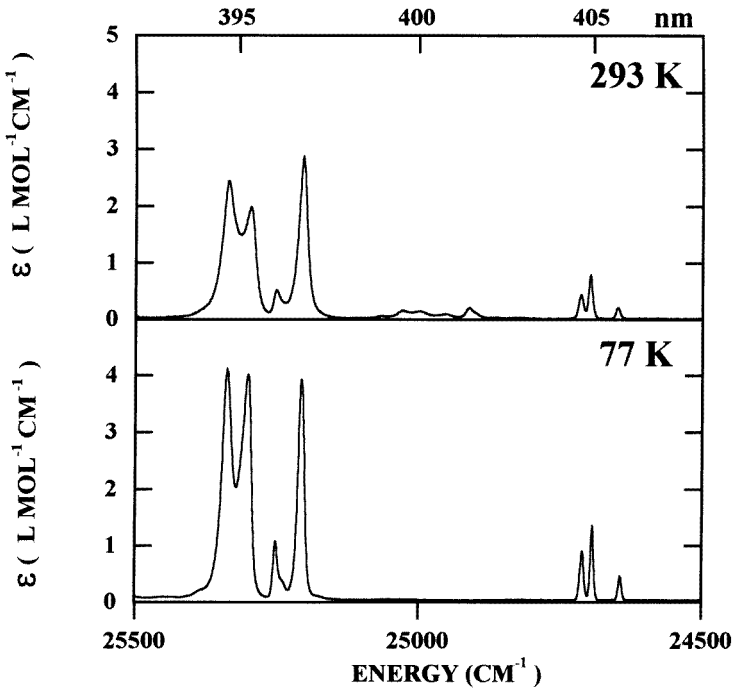

Figure 6. Absorption spectra of the transition to $^5L_6$ in YGG:Eu^{3+} at 293 and at 77 K.

Between 25 500 and 27 200 cm^{-1}, transitions to the multiplets $^5L_7$, $^5L_8$, $^5G_2$, $^5G_3$, $^5G_4$, $^5G_5$ and $^5G_6$ are located. This spectral region is very congested and assignments are only possible by comparing the experimental and calculated crystal-field levels. Transitions starting from the $^7F_0$ and the first excited state $^7F_1$ overlap. Spectra at different temperatures are thus necessary. Because of the high density of crystal-field levels, the Russell–Saunders coupling scheme cannot give an adequate description of the free-ion levels. Affixing a $^{2S+1}L_J$ label to a transition is not possible without ambiguity. Often, the Russell–Saunders notation of the wave function component with the largest coefficient is chosen as the

label, but this is a difficult task in the presence of several components with nearly equal coefficients.

In YGG:Eu^{3+}, not only do the $^5D_4$ and $^5L_9$ manifolds overlap energetically, but their wave functions are mixed too. If there was the choice between assigning a level to the $^5D_4$ or to the $^5L_9$ manifold, the assignment to $^5D_4$ was preferred because these transitions are more likely to occur than transitions to $^5L_9$ (with respect to the selection rules for induced electric dipole transitions). These transitions are found between 27 450 and 27 700 cm^{-1} (figure 7). Between 27 880 and 28 670 cm^{-1}, four very weak crystal-field transitions are observed and these can be assigned to the $^5L_{10} \leftarrow {}^7F_0$ transition. The $^5L_{10} \leftarrow {}^7F_0$ is only found for Eu^{3+} systems with a strong crystal-field interaction, which results in a strong J-mixing.

A high density of states is observed for the transitions to the ^5H_J multiplets ($J = 3$, 4, 5, 6, 7): 55 crystal-field levels are calculated inside a spectral region between 30 700 and 32 000 cm^{-1}. One can expect thus a strong violation of the Russell–Saunders coupling scheme and difficulties in affixing a $^{2S+1}L_J$ label to the transitions. 15 crystal-field levels are detected experimentally. Assignment can be made only after a detailed energy level calculation. Above 32 000 cm^{-1}, no intraconfigurational 4f–4f transitions of Eu^{3+} could be detected, because of a strong absorption by the garnet host matrix. The transitions are summarized in table 1.

4. Energy level calculations

The total Hamiltonian can be written as a free-ion part and a crystal-field part:

$$H = H_{free\ ion} + H_{crystal\ field}. \tag{1}$$

The free-ion Hamiltonian is characterized by a set of three electron repulsion parameters (F^2, F^4, F^6), the spin–orbit coupling constant ζ_{4f}, the Trees configuration interaction parameters (α, β, γ), the three-body configuration interaction parameters ($T^2, T^3, T^4, T^6, T^7, T^8$) and parameters which describe magnetic interactions ($M^0, M^2, M^4, P^2, P^4, P^6$). A further parameter E_{ave} takes the kinetic energy of the electrons and their interactions with the nucleus into account. It shifts only the barycentre of the whole 4f configuration, so one can write [6]

$$H_{free\ ion} = E_{ave} + \sum_k F^k f_k + \zeta_{4f} A_{so} + \alpha L(L+1) + \beta G(G_2) + \gamma G(R_7) + \sum_i T^i t_i + \sum_k P^k p_k + \sum_l M^l m_l \tag{2}$$

$i = 2, 3, 4, 6, 7, 8 \qquad k = 2, 4, 6 \qquad l = 0, 2, 4.$

f_k and A_{so} represent the angular part of the electrostatic and spin–orbit interaction respectively. L is the total orbital angular momentum. $G(G_2)$ and $G(R_7)$ are the Casimir operators for the groups G_2 and R_7. The t_i are the three-particle operators. p_k and m_l represent the operators for the magnetic corrections.

The crystal-field Hamiltonian is given by

$$H_{crystal\ field} = -eV \tag{3}$$

where e is the elementary charge and V the crystal-field potential. For a D_2 symmetry, the even part of the crystal-field potential is expanded as [7]

$$V^{even}(D_2) = B_0^2 C_0^2 + B_2^2 (C_{-2}^2 + C_2^2) + B_0^4 C_0^4 + B_4^4 (C_{-4}^4 + C_4^4) + B_2^4 (C_{-2}^4 + C_2^4) + B_0^6 C_0^6 + B_2^6 (C_{-2}^6 + C_2^6) + B_4^6 (C_{-4}^6 + C_4^6) + B_6^6 (C_{-6}^6 + C_6^6). \tag{4}$$

Table 1. Transition energies (cm^{-1}) in the absorption spectra of $Y_3Ga_5O_{12}$:Eu^{3+}. Transitions which are only detected in the spectra at ambient temperature are marked with an asterisk (∗). The transitions are labelled according to the $^{2S+1}L_J$ Russell–Saunders term with largest coefficient in the total wave function.

No	Energy (cm^{-1})	Transition	No	Energy (cm^{-1})	Transition
1*	4616	$^7F_6 \leftarrow ^7F_1$	52*	24 954	$^5L_6 \leftarrow ^7F_1$
2*	4689	$^7F_6 \leftarrow ^7F_1$	53*	24 999	$^5L_6 \leftarrow ^7F_1$
3*	4760	$^7F_6 \leftarrow ^7F_1$	54*	25 029	$^5L_6 \leftarrow ^7F_1$
4*	4852	$^7F_6 \leftarrow ^7F_1$	55*	25 066	$^5L_6 \leftarrow ^7F_1$
5*	4881	$^7F_6 \leftarrow ^7F_1$	56	25 206	$^5L_6 \leftarrow ^7F_0$
6*	4960	$^7F_6 \leftarrow ^7F_1$	57	25 239	$^5L_6 \leftarrow ^7F_0$
7	5001	$^7F_6 \leftarrow ^7F_0$	58	25 251	$^5L_6 \leftarrow ^7F_0$
8	5017	$^7F_6 \leftarrow ^7F_0$	59	25 302	$^5L_6 \leftarrow ^7F_0$
9	5028	$^7F_6 \leftarrow ^7F_0$	60	25 338	$^5L_6 \leftarrow ^7F_0$
10	5035	$^7F_6 \leftarrow ^7F_0$	61*	25 599	$^5L_7 \leftarrow ^7F_1$
11	5076	$^7F_6 \leftarrow ^7F_0$	62*	25 644	$^5L_7 \leftarrow ^7F_1$
12	5103	$^7F_6 \leftarrow ^7F_0$	63	25 694	$^5L_7 \leftarrow ^7F_0$
13	5224	$^7F_6 \leftarrow ^7F_0$	64	25 703	$^5L_7 \leftarrow ^7F_0$
14	5256	$^7F_6 \leftarrow ^7F_0$	65	25 731	$^5L_7 \leftarrow ^7F_0$
15*	16 406	$^5D_0 \leftarrow ^7F_2$	66	25 742	$^5L_7 \leftarrow ^7F_0$
16*	16 820	$^5D_0 \leftarrow ^7F_1$	67*	25 800	$^5L_7 \leftarrow ^7F_1$
17*	16 867	$^5D_0 \leftarrow ^7F_1$	68*	25 833	$^5L_7 \leftarrow ^7F_1$
18*	16 902	$^5D_0 \leftarrow ^7F_1$	69*	25 887	$^5L_7 \leftarrow ^7F_1$
19*	18 567	$^5D_1 \leftarrow ^7F_1$	70*	25 907	$^5L_7 \leftarrow ^7F_1$
20*	18 627	$^5D_1 \leftarrow ^7F_1$	71	25 980	$^5G_2 \leftarrow ^7F_0$
21*	18 611	$^5D_1 \leftarrow ^7F_1$	72	26 023	$^5G_2 \leftarrow ^7F_0$
22	18 954	$^5D_1 \leftarrow ^7F_0$	73*	26 074	$^5G_3 \leftarrow ^7F_1$
23	18 971	$^5D_1 \leftarrow ^7F_0$	74*	26 105	$^5G_3 \leftarrow ^7F_1$
24*	21 037	$^5D_2 \leftarrow ^7F_1$	75	26 136	$^5L_7 \leftarrow ^7F_0$
25*	21 061	$^5D_2 \leftarrow ^7F_1$	76	26 191	$^5L_7 \leftarrow ^7F_0$
26*	21 082	$^5D_2 \leftarrow ^7F_1$	77	26 269	$^5G_4 \leftarrow ^7F_0$
27*	21 107	$^5D_2 \leftarrow ^7F_1$	78	26 296	$^5G_3 \leftarrow ^7F_0$
28*	21 143	$^5D_2 \leftarrow ^7F_1$	79	26 314	$^5G_3 \leftarrow ^7F_0$
29	21 362	$^5D_2 \leftarrow ^7F_0$	80	26 340	$^5L_7 \leftarrow ^7F_0$
30	21 448	$^5D_2 \leftarrow ^7F_0$	81	26 387	$^5G_2 \leftarrow ^7F_0$
31	21 471	$^5D_2 \leftarrow ^7F_0$	82	26 478	$^5L_8 \leftarrow ^7F_0$
32*	23 883	$^5D_3 \leftarrow ^7F_1$	83	26 491	$^5L_8 \leftarrow ^7F_0$
33*	23 828	$^5D_3 \leftarrow ^7F_1$	84	26 523	$^5G_6 \leftarrow ^7F_0$
34*	23 843	$^5D_3 \leftarrow ^7F_1$	85	26 631	$^5G_6 \leftarrow ^7F_0$
35*	23 873	$^5D_3 \leftarrow ^7F_1$	86	26 664	$^5G_5 \leftarrow ^7F_0$
36*	23 908	$^5D_3 \leftarrow ^7F_1$	87	26 677	$^5G_5 \leftarrow ^7F_0$
37*	23 924	$^5D_3 \leftarrow ^7F_1$	88	27 144	$^5L_8 \leftarrow ^7F_0$
38*	23 953	$^5D_3 \leftarrow ^7F_1$	89	27 158	$^5G_8 \leftarrow ^7F_0$
39	24 214	$^5D_3 \leftarrow ^7F_0$	90*	27 188	$^5D_4 \leftarrow ^7F_1$
40	24 230	$^5D_3 \leftarrow ^7F_0$	91*	27 228	$^5D_4 \leftarrow ^7F_1$
41	24 243	$^5D_3 \leftarrow ^7F_0$	92	27 263	$^5L_8 \leftarrow ^7F_0$
42	24 284	$^5D_3 \leftarrow ^7F_0$	93	27 492	$^5D_4 \leftarrow ^7F_0$
43	24 295	$^5D_3 \leftarrow ^7F_0$	94	27 506	$^5L_9 \leftarrow ^7F_0$
44	24 300	$^5D_3 \leftarrow ^7F_0$	95	27 516	$^5D_4 \leftarrow ^7F_0$
45*	24 342	$^5L_6 \leftarrow ^7F_1$	96	27 560	$^5D_4 \leftarrow ^7F_0$
46*	24 392	$^5L_6 \leftarrow ^7F_1$	97	27 571	$^5D_4 \leftarrow ^7F_0$
47*	24 411	$^5L_6 \leftarrow ^7F_1$	98	27 596	$^5D_4 \leftarrow ^7F_0$
48	24 643	$^5L_6 \leftarrow ^7F_0$	99	28 417	$^5L_{10} \leftarrow ^7F_0$
49	24 693	$^5L_6 \leftarrow ^7F_0$	100	28 482	$^5L_{10} \leftarrow ^7F_0$
50	24 710	$^5L_6 \leftarrow ^7F_0$	101	28 614	$^5L_{10} \leftarrow ^7F_0$
51*	24 912	$^5L_6 \leftarrow ^7F_1$	102	28 694	$^5L_{10} \leftarrow ^7F_0$

Table 1. (Continued)

No	Energy (cm^{-1})	Transition	No	Energy (cm^{-1})	Transition
103	30 760	$^5H_3 \leftarrow ^7F_0$	111	31 273	$^5H_4 \leftarrow ^7F_0$
104	30 810	$^5H_7 \leftarrow ^7F_0$	112	31 294	$^5H_4 \leftarrow ^7F_0$
105	30 967	$^5H_4 \leftarrow ^7F_0$	113	31 387	$^5H_6 \leftarrow ^7F_0$
106	30 987	$^5H_3 \leftarrow ^7F_0$	114	31 460	$^5H_6 \leftarrow ^7F_0$
107	31 014	$^5H_3 \leftarrow ^7F_0$	115	31 594	$^5H_6 \leftarrow ^7F_0$
108	31 064	$^5H_7 \leftarrow ^7F_0$	116	31 632	$^5H_6 \leftarrow ^7F_0$
109	31 213	$^5H_4 \leftarrow ^7F_0$	117	31 638	$^5H_6 \leftarrow ^7F_0$
110	31 234	$^5H_4 \leftarrow ^7F_0$			

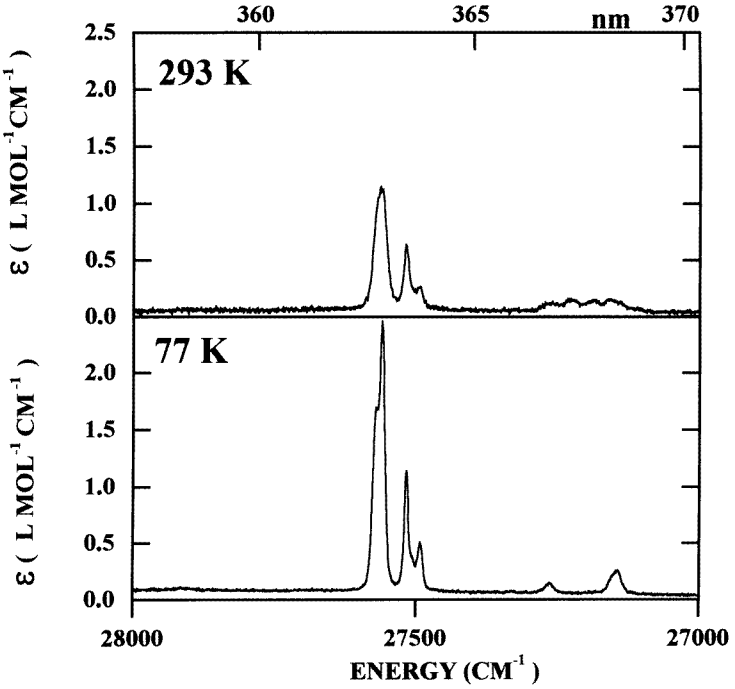

Figure 7. Absorption spectra of the transitions to $^5D_4$, $^5L_9$ and $^5L_8$ in YGG:Eu^{3+} at 293 and at 77 K.

The C_q^k are spherical tensor operators of rank k, with components q. The B_q^k are the crystal-field parameters. The crystal-field parametrization of the garnet systems is more complicated than the parametrization of other systems, because of the six non-equivalent D_2 sites (see the introduction). Three choices of the z-axis are possible in a D_2 symmetry. For each of the three choices, one has two possible orientations, which only affect the signs of the $q = \pm 2$ and $q = \pm 4$ components. Six equivalent sets of crystal-field parameters can be defined. These sets may appear completely different, but they give an identical crystal-field splitting. The relations between the equivalent sets of crystal-field parameters are given by Morrison and Leavitt [2]. We have chosen arbitrarily the set 3 orientation of Morrison and Leavitt for our crystal-field parametrization.

Table 2. Optimized free-ion and crystal-field parameters (cm^{-1}) for Eu^{3+} in $Y_3Ga_5O_{12}$ (D_2 symmetry). The errors on the parameters are given in parentheses. Parameters which were constrained during the fitting produce are placed in square brackets. $\sigma = 14.8$ cm^{-1}.

Parameter	Value (cm^{-1})	Parameter	Value (cm^{-1})
E_{ave}	63 669 (17)	M^0	2.594 (0.084)
F^2	82 347 (57)	M^2	$[0.56M^0]$
F^4	59 844 (69)	M^4	$[0.38M^0]$
F^6	42 359 (43)	P^2	[303]
α	19.088 (0.723)	P^4	$[0.75P^2]$
β	−612 (9)	P^6	$[0.50P^2]$
γ	1456 (7)	B_0^2	−40 (27)
T^2	416 (5)	B_2^2	153 (23)
T^3	[40]	B_0^4	−1990 (40)
T^4	[40]	B_2^4	230 (42)
T^6	[−330]	B_4^4	1124 (31)
T^7	[380]	B_0^6	1054 (60)
T^8	[370]	B_2^6	−192 (41)
ζ_{4f}	1333.78 (1.81)	B_4^6	1459 (44)
		B_6^6	−248 (44)

The parameter set is determined by optimizing a starting set. This is done by minimizing the squares of the differences between the experimental and calculated crystal-field levels. The ^7F_J levels ($J = 2$–5) are taken from the article by Koningstein [3]. The parameters T^3, T^4, T^6, T^7, T^8, P^2, P^4 and P^6 were constrained during the fitting procedure. The M^l and P^k parameters are in the pseudo-relativistic Hartree–Fock ratios $M^2/M^0 = 0.56$, $M^4/M^0 = 0.38$, $P^4/P^2 = 0.75$ and $P^6/P^2 = 0.50$ [8]. The r.m.s. value (σ-value) of the last fit was 14.8 cm^{-1}. The final parameter set can be found in table 2. In table 3, the experimental and calculated crystal-field levels are given.

5. Discussion and conclusions

The agreement between calculated and experimental energy levels is good. It was however necessary to take J-mixing into account. The J-mixing is enhanced by the strong crystal field in the garnet host, in comparison with other single-crystal hosts. Because of the J-mixing, several transitions starting from the $^7F_0$ ground state and not obeying the selection rule $\Delta J = 2, 4, 6$ for induced electric dipole transitions are observed. Examples are the transitions from $^7F_0$ to $^5D_3$, $^5L_8$, $^5L_9$ and $^5L_{10}$.

The absorption spectra of YGG:Eu^{3+} and YAG:Eu^{3+} [9] are very similar, although it should be remarked that the ultraviolet cut-off is at a lower energy for YGG than for YAG. This similarity can be expected, because of the structural relationship between the two matrices (both have the garnet structure). The same crystal-field transitions and the same free-ion $^{2S+1}L_J$ manifolds are observed. The crystal-field strengths in the two host crystals are not identical however. The magnitude of the crystal-field splitting of the $J = 1$ levels is greatly reduced in YGG:Eu^{3+} compared to the magnitude of the crystal-field splitting in YAG:Eu^{3+}. The total crystal-field splitting of the $^7F_1$ level is 172 cm^{-1} in YAG:Eu^{3+}, but only 82 cm^{-1} in YGG:Eu^{3+}. For $^5D_1$, the splitting is 39 cm^{-1} in YAG:Eu^{3+} and 16 cm^{-1} in YGG:Eu^{3+}. The values of the $k = 2$ crystal-field parameters are therefore smaller in

Table 3. Experimental and calculated energy levels (cm^{-1}) of Eu^{3+} in $Y_3Ga_5O_{12}$ (D_2 symmetry).

$^{2S+1}L_J$	μ	E_{exp} (cm^{-1})	E_{calc} (cm^{-1})	$E_{exp} - E_{calc}$ (cm^{-1})
$^7F_0$	0	0	5	−5
$^7F_1$	±1	308	317	−9
	0	343	355	−12
	±1	390	409	−19
$^7F_2$	±1	—	811	—
	±1	—	820	—
	0	829	826	+3
	0	—	1318	—
	0	—	1326	—
$^7F_3$	±1	—	1828	—
	0	1882	1867	+15
	±1	1896	1891	+5
	±1	1950	1963	−7
	0	1982	1969	+13
	±1	2004	1982	+22
	0	—	2184	—
$^7F_4$	0	—	2385	—
	±1	2851	2839	+12
	0	—	2869	—
	±1	2935	2914	+15
	±1	3073	3089	−16
	±1	3083	3096	−13
	0	3108	3109	−1
	0	—	3162	—
	0	3202	3201	+1
$^7F_5$	±1	3758	3762	−4
	0	3788	3798	−10
	±1	—	3807	—
	±1	3984	3966	+22
	±1	4026	4026	0
	0	4042	4034	+8
	0	4150	4153	−3
	±1	—	4184	—
	±1	—	4203	—
	0	—	4219	—
	0	—	4241	—
$^7F_6$	0	5001	4979	+22
	±1	5017	5020	−3
	0	5028	5039	−11
	±1	—	5046	—
	±1	—	5055	—
	0	5076	5091	−15
	±1	5103	5102	+1
	0	5224	5255	−31
	0	—	5255	—
	±1	5231	5263	−32
	0	—	5270	—
	0	—	5273	—
	±1	—	5279	—
$^5D_0$	0	17 210	17 201	+9
$^5D_1$	±1	18 954	18 941	+9
	0	18 954	18 951	+3
	±1	18 970	18 971	−1
$^5D_2$	0	21 344	21 371	−27
	0	21 362	21 374	−12
	±1	21 451	21 442	+9
	0	—	21 451	—
	±1	21 471	21 459	+12

Table 3. (Continued)

$^{2S+1}L_J$	μ	E_{exp} (cm^{-1})	E_{calc} (cm^{-1})	$E_{exp} - E_{calc}$ (cm^{-1})
$^5D_3$	± 1	24 214	24 228	−14
	0	24 231	24 242	−11
	± 1	24 244	24 262	−18
	0	24 284	24 277	+ 7
	± 1	24 296	24 283	+ 13
	± 1	—	24 284	—
	0	24 300	24 297	+ 3
$^5L_6$	0	24 643	24 651	−8
	0	—	24 665	—
	± 1	24 693	24 693	0
	± 1	—	24 694	—
	0	24 710	24 707	+ 3
	0	—	24 718	—
	± 1	25 206	25 192	+ 14
	0	—	25 195	—
	± 1	25 239	25 238	+ 1
	± 1	25 251	25 265	−14
	0	25 302	25 281	+ 21
	± 1	25 338	25 315	+ 23
	0	25 374	25 379	−5
(a)				
$^5D_4$, $^5L_9$	± 1	27 492	27 487	+ 5
	0	27 506	27 509	+ 3
	± 1	—	27 522	—
	0	27 516	27 533	−17
	0	—	27 538	+ 10
	± 1	—	27 547	—
	± 1	27 560	27 553	+ 7
	0	—	27 565	—
	0	—	27 565	—
	± 1	—	27 567	—
	± 1	27 571	27 579	−8
	0	27 596	27 592	+ 4
	± 1	—	27 633	—
	0	—	27 642	—
(b)				
$^5H_{3,4,5,6,7}$	0	30 760	30 718	+ 42
	± 1	30 810	30 831	−21
	± 1	30 967	30 984	−17
	± 1	30 987	30 990	−3
	0	31 014	31 001	+ 13
	0	31 064	31 036	+ 28
	0	31 213	31 216	−3
	± 1	31 234	31 249	−15
	± 1	31 273	31 266	+ 7
	0	31 294	31 299	−5
	± 1	31 387	31 403	−16
	± 1	31 460	31 453	+ 7
	± 1	31 594	31 599	−5
	0	31 632	31 614	+ 18
	0	31 638	31 645	−7

(a) Between 25 690 and 27 370 cm^{-1}, 77 crystal-field levels of the multiplets $^5L_7$, $^5L_8$, $^5G_2$, $^5G_3$, $^5G_4$, $^5G_5$ and $^5G_6$ are calculated. 22 are observed in the spectra.
(b) Between 27 880 and 28 670 cm^{-1}, 35 crystal-field levels belonging to $^5L_9$ and $^5L_{10}$ are calculated. Only four of them are found in the spectra.

YGG:Eu^{3+} ($B_0^2 = -40$ cm^{-1}, $B_2^2 = 153$ cm^{-1}) than in YAG:Eu^{3+}($B_0^2 = -263$ cm^{-1}, $B_2^2 = 284$ cm^{-1}). The smaller value for the parameter B_0^2 can be rationalized in terms of a smaller deviation from a cubic coordination polyhedron in YGG than in YAG. The difference in the splitting is less pronounced in the other $^{2S+1}L_J$ manifolds. Therefore, the $k = 4$ and $k = 6$ parameters are nearly the same in the two matrices (compare with the values of [9]). The total crystal-field splitting of $^5D_2$ is 121 cm^{-1} in YAG:Eu^{3+} and 127 cm^{-1} in YGG:Eu^{3+}. The splitting of the $^5L_6$ manifold is 768 cm^{-1} in YAG:Eu^{3+} and 731 cm^{-1} in YGG:Eu^{3+}. The crystal-field levels of $^5L_6$ are in YGG:Eu^{3+} also divided into two subgroups, just as in YAG:Eu^{3+}.

Acknowledgments

KB is a postdoctoral fellow of the Belgian National Fund for Scientific Research (NFWO). Financial support from the Geconcerteerde Onderzoeksakties (Konventie No 87 93-110) and from the IIKW (4.0007.94 and G.0124.95) is gratefully acknowledged. We wish to thank G Blasse (University of Utrecht, The Netherlands) for providing us with the YGG:Eu^{3+} single crystal.

References

[1] Weber M J 1979 Rare-earth lasers *Handbook on the Physics and Chemistry of Rare-earths* vol 4, ed K A Gschneidner Jr and L Eyring (Amsterdam: North-Holland) ch 35, p 275
[2] Morrison C A and Leavitt R P 1982 Spectroscopic properties of triply ionized lanthanides in transparent host crystals *Handbook on the Physics and Chemistry of Rare-earths* vol 5, ed K A Gschneidner Jr and L Eyring (Amsterdam: North-Holland) ch 46, p 461
[3] Koningstein J A 1965 *J. Chem. Phys.* **42** 3195
[4] Dillon J F Jr and Walker L R 1961 *Phys. Rev.* **124** 1401
[5] Binnemans K and Görller-Walrand C 1995 *Chem. Phys. Lett.* **235** 163
[6] Carnall W T, Goodman G L, Rajnak K and Rana R S 1989 *J. Chem. Phys.* **90** 3443
[7] Wybourne B G 1965 *Spectroscopic Properties of Rare-earths* (New York: Wiley)
[8] Judd B R and Crosswhite H 1984 *J. Opt. Soc. Am.* B **1** 255
[9] Binnemans K and Görller-Walrand C 1996 *J. Chem. Soc.: Faraday Trans.* **92** 2487